THE ROLE OF DUPLEX TREATMENT TO INCREASING THE CAVITATION EROSION RESISTANCE FOR STEELS USED IN MANUFACTURING HYDRAULIC EQUIPMENT

Doctoral thesis – Summary
to obtain the scientific title of doctor (PhD) at
Politehnica University of Timişoara
in the doctoral domain of Materials Engineering

author ing. Cristian GHERA
scientific advisers Prof.univ.dr.ing. Ion MITELEA
Prof.univ.dr.ing.Ilare BORDEAŞU
Timişoara 2017

1. Current state of cavitation research in the hydraulic drive systems

The hydraulic drives represent an important domain of the modern technology, with a wide applicability, which has penetrated almost all industrial branches, from the energy field, machine building, machine tools, auto, aviation, naval, medicine to aerospace industry.

Combined with the electric drives and various automated systems, hydraulic systems can handle extremly diverse working regimes, which is why they will benefit from a wider range of interest in terms of both practical applicability and research.

The hydraulic systems of hydrostatic type [2, 8], according to Fig. 1.2, have the role of transforming, through hydraulic apparatus, the electrical or mechanical energy (typically produced by standard motors) in hydraulic energy (in the form of pressurized fluid), to control and distribute it at points of interest, and to convert it to mechanical energy, to the necessary parameters.

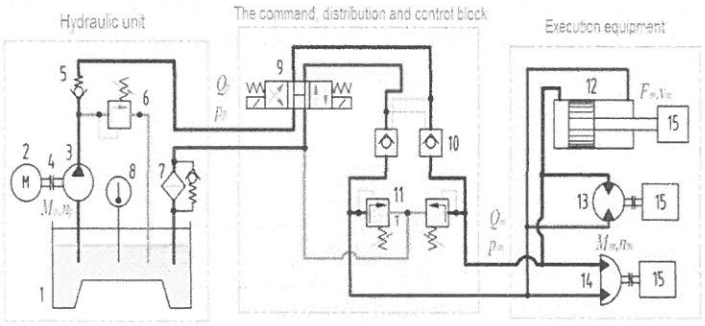

Fig.1.1. The structure of a hydraulic system

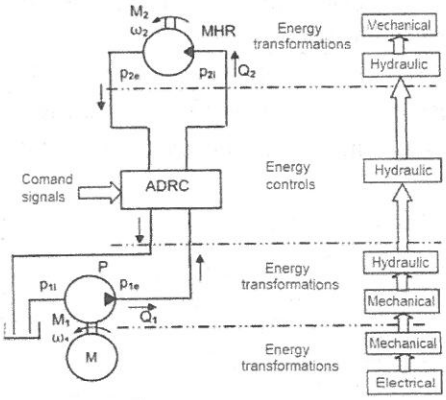

Fig.1.2. Energy transformation in hydraulic drive systems of hydrostatic type

In general, as shown in Fig. 1.1, the hydrostatic drive systems consist of a hydraulic unit (which generates a liquid flow Q_p at a pressure p_p), a command, distribution and control block, and the execution equipment, which can be fixed mountedor on mobile machinery.

The global tendencies of reducing the gauge of the hydraulic apparatus have the effect of increasing the working speeds through them, which results in decreasing the pressure value

in the interstices to the vapor pressure value, and implicity the initiation of the cavitation phenomenon [1-3, 7-9, 19].

The researches done in the Lausanne Federal Polytechnic School's Laboratories,Fig. 1.3, through ultrasound camera (37500 frames / second) and 3D modelling, provide the way of cavitation bubble formation, development, and propagation of microjets and shock waves, which cause the deterioration of solid borders in the immediate vicinity.

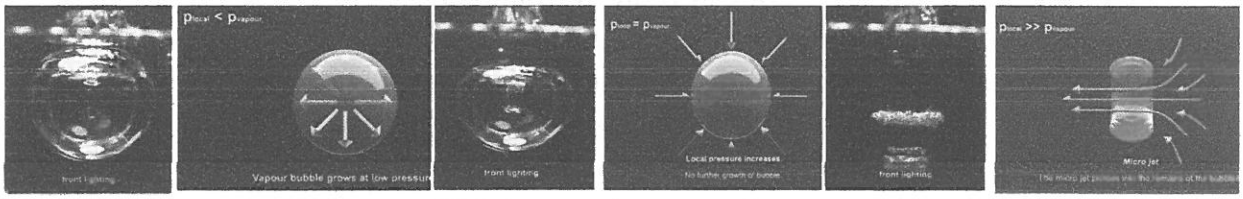

Fig.1.3. The formation and implosion of cavitation bubbles [20]

The erosion effects are visible both on the mobile elements and on the body of the devices, Fig. 1.4.

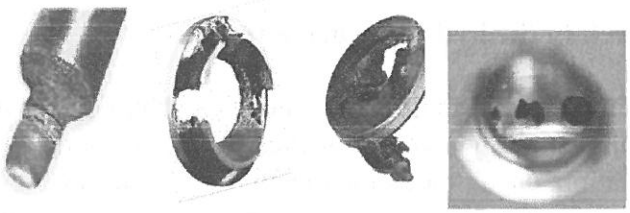

Fig.1.4. Elements of hydraulic apparatures, damaged by cavitation

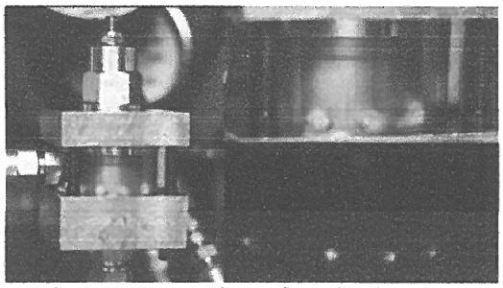

Fig.1.5. Formation of cavitational areas, accompanied by the phenomenon of sonoluminescence

The hydraulic equipment manufacturing company Sun Hydraulics, Fig 1.5, has highlighted both cavitation bubble formation areas and the sonoluminescence phenomenon which accompanies their implosion, in the pressure-operated valves, cartridge type, as shown in the picture.

The susceptible areas to the occurrence and development of cavitation in the main hydraulic apparatus [3, 12], namely in the directional valve with linear drawer, respectively conical valve pressure control valves, are show in Fig. 1.6 and 1.7.

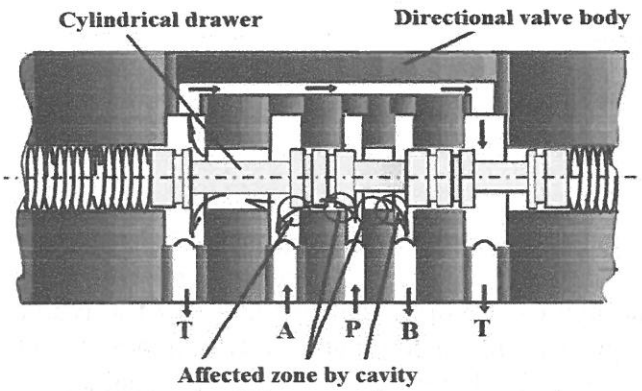

Fig.1.9. Susceptible areas of occurrence and development of cavitation in the directional valve with linear drawer

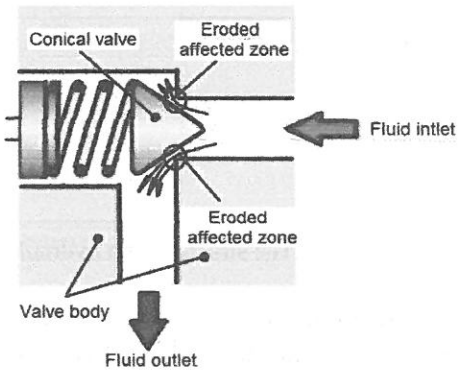

Fig.1.10. Susceptible areas to cavitation development and development in the pressurre regulation valves with conical valve

Objectives of the doctoral thesis

1. Improvement of cavitation resistance of low-alloy steels treated with Duplex by carburizing followed by surface hardening by induction;
2. Investigation of thermal annealing treatment followed by work hardening with laser beam in the increase of cavitation resistance of the low-alloyed steel 16MnCr5;
3. Increase of cavitation resistance by heat treatment for hardening and tempering, followed by gas nitriding or laser nitriding of the alloy steel 34CrNiMo6;
4. The establishment of a new procedure for assessing the resistance of steels to cavitation erosion, based on the roughness parameter R_z.

The novelty of the theme consists in the fact it studies techniques specific to the Duplex type combined treatment, which aim to sum up the superior mechanical and structural characteristics obtained by each treatment in order to improve their behavior to the vibratory cavitation erosion, of two widely used steels in the construction of hydraulic components.

The amplification of studies regarding the causes which determine the cavitation in the hydraulic drive systems, especially in the control, distribution and adjustment devices, and finding of solutions to ensure a good dynamic functioning, is a necessity. These studies are also desirable because vibrations caused by the typical cycle of evolution of individual and clustered cavitational bubbles can be extended to the entire assembly of pipes, machines and execution motors (linear / rotary), a particularity serious phenomenon in the automated hydraulic systems.

2. Investigated materials. Used laboratory equipment. Methods of analysis and evaluation.

The researches in the doctoral thesis were made on two steels, designed for the manufacture of mobile parts from the hydraulic control, distribution and regulation apparatus, which, under certain operating regimes, are subjected to the destructive attack of microjets and shock waves created by the cavitation bubble implosion; namely 16MnCr5, respectively the improved alloy steel 34CrNiMo6.

The low-alloyed steel 16MnCr5 – alphanumerical symbolized 1.7131 according to the Standard EN 10084:2008, is a hypoeutectoid steel [3, 10, 11, 15, 16] for carburation with the chemical composition shown in Table 2.1, and the mechanical characteristics presented in Table 2.2.

Table 2.1. Chemical composition of the steel 16MnCr5 (No.:1.7131)

Material 16MnCr5	Elemente însoțitoare și de aliere, %							
	C	Si	Mn	Cr	P	S	Mo	Fe
Prescribed values	0.14÷ 0,19	max. 0,40	1÷ 1.3	0.8÷ 1,1	max. 0,025	max. 0,035	-	rest
Effective values	0.16	0.28	1.06	1.12	0.010	0.026	0.02	rest

Table 2.2. Mechanical characteristics of the steel 16MnCr5 in the annealed state

Material 16MnCr5	Rm N/mm^2	$Rp_{0.2}$ N/mm^2	A_5 %	Z %	HV daN/mm^2
Prescribed values	550	420	21	62÷64	170
Effective values	560	425	20	62	185

The low-alloyed steel 34CrNiMo6 – alphanumerical symbolized 1.6582 according to the Standard EN 10083-3:2006, is a hypoeutectoid steel with a wide applicability range in the hydraulic apparatus and not only [3, 13, 15, 17] with the chemical composition shown in Table 2.3, and the mechanical characteristics presented in Table 2.4.

Table 2.3. Chemical composition of the alloy steel 34CrNiMo6 (No.:1.6582)

Marca 34CrNiMo6	Elemente însoţitoare şi de aliere, %							
	C	Si	Mn	Cr	Ni	P	S	Mo
Prescribed values	0,3÷ 0,38	max. 0,4	0,5÷ 0,8	1,3÷ 1,7	1,3÷ 1,7	max. 0,025	max. 0,035	0,15 ÷0,3
Effective values	0,34	0,25	0,61	1,34	1,45	0,008	0,019	0,18

Table 2.4. Mechanical characteristics of the steel in hardening and tempering state

Material 34CrNiMo6	Rm N/mm^2	$Rp_{0.2}$ N/mm^2	A5 %	Z %	HB daN/mm^2
Prescribed values	1100÷1300	900	9-14	45	248÷255
Effective values	1300	1000	9	45	249

The alloyed steel 41Cr4 – standard steel – alphanumerical symbolized 1.7035, is a hypoeutectoid steel, with a wide applicability in the construction of hydraulic apparatus [3], taken as a reference due to its good resistance to cavitation erosion, having the chemical composition and mechanical characteristics presented in Tables 2.5 and 2.6 according to the European Standards, respectively the average, according to the quality certificate issued by the manufacturer.

Tabel 2.5. Chemical composition of the alloy steel41Cr4 (No.:1.7035)

Marca 41Cr4	Elemente însoţitoare şi de aliere, %					
	C	Si	Mn	Cr	P	S
Prescribed values	0,38÷ 0,45	max. 0,4	0,6÷ 0,9	0,9÷ 1,2	max. 0,025	max. 0,035
Effective values	0.42	0,25	0.70	1.05	0,025	0,03

Tabel 2.6. Mechanical characteristics of the steel in hardening and tempering state

Material 41Cr4	Rm N/mm^2	$Rp_{0.2}$ N/mm^2	A5 %	Z %	HB daN/mm^2
Prescribed values	900÷1100	660	12	35	241÷255
Effective values	1000	660	12	35	255

The cavitation tests were conducted in the Cavitation Laboratory of Politehnica University of Timişoara, on a standard vibratory apparatus with piezoceramic crystals,Fig. 2.1, on samples made from the investigated materials, subjected to different combinations of thermal and thermochemical treatments [3-5, 10-13, 16-18, 19].

The mass losses were determined by weighing on the analitycal balance with an accuracy of 10^{-5} g, Fig. 2.2, and the roughness measurements were made using the Mitutoyo digital rugosimeter.

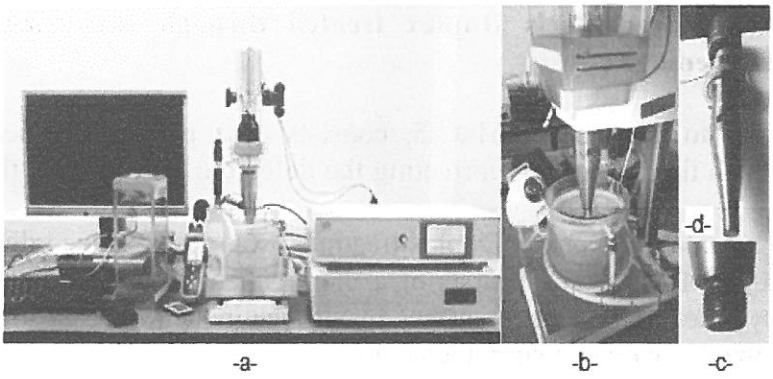

-a- -b- -c-

Fig.2.1. Vibratory apparatus with piezoceramic crystals

Fig.2.2. Analitycal balance type Zatklady Mechaniki Precyzyjnej WP1

The microstucrtural investigations were done in the Materials Engineering Laboratory, using the provided equipment, such as the optical microscope, Fig. 2.4, the scanning electron microscope, Fig. 2.3, for capturing enlarged images at different scales and the determination of the chemical elements by dispersion analysis in energy and X-rays; Vickers microhardness, Fig. 2.6, for hardness measurements; respectively the X-ray diffractometer, brand X'Pert from the Phillips firm, Fig. 2.5 for the determination of the existent phases by X-ray diffraction analysis.

Fig.2.3. Scanning electron microscope TESCAN VEGA 3 LMU Bruker EDX Quantax

Fig.2.4. Microscope OPLIMPUS SYX7

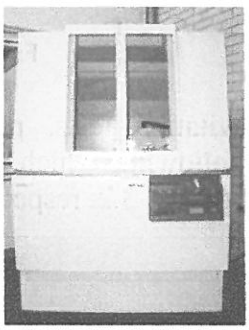

Fig.2.5. X-ray diffractometer (X'Pert from the Philips firm)

Fig.2.6 Digital microhardness Vikers HV-50AC

The selected materials for experimentation are intended for the manufacturing of mobile parts in hydraulic, command, distribution and control equipment (drawers, valves, etc.) [3], which, under certain operating modes, are subjected to the destructive attack of microjets and shock waves created by the cavitation bubble implosion.

The apparatus and methods of experimentation/investigation correspond to the standard requirements for conducting the scientific research.

The evaluation methods of the behavior and resistance to the vibratory cavitation erosion and investigation of the eroded structures are in accordance with the Standards, being used in the Laboratories of Cavitation and Materials Engineering of the Politehnica University of Timişoara.

3. Cavitation resistance of low-alloyed steels Duplex treated through carburizing followed by surface induction hardening.

The first applied treatment to the steel 16MnCr5, consists of a preliminary heat treatment by annealing [14, 15] with the purpose of correcting the defective structures of the material.

Subsequently to the mechanical processing, a Duplex treatment was applied, according to the cyclogram of Fig. 3.1 [4, 11, 15], which consists of a thermochemical treatment by carburization in gas, followed by a heat treatment of surface by surface induction hardening, and tempering, having as a resultthe decrease of internal tensions.

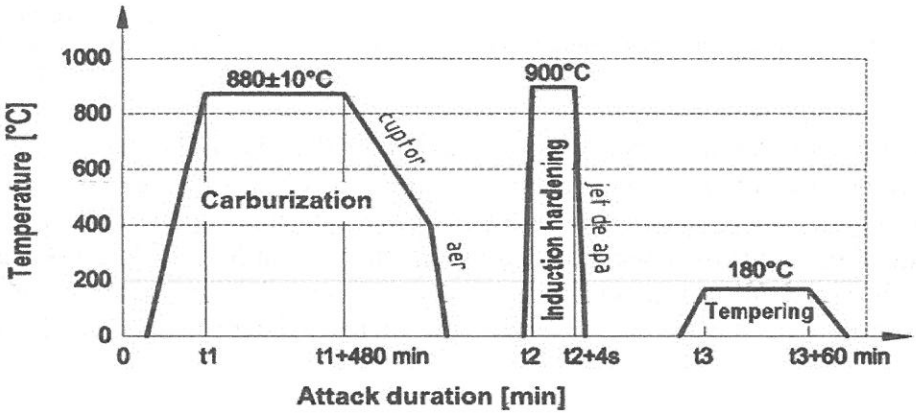

Fig.3.1. Duplex treatment cyclogram

The cavitation tests, performed according to the ASTM G32-2010 normative requirements, following which specific characteristic curves were raised: Mean Depth of Erosion MDE (t), Fig. 3.2, respectively Mean Depth of Erosion Rate MDER(t), Fig. 3.3.

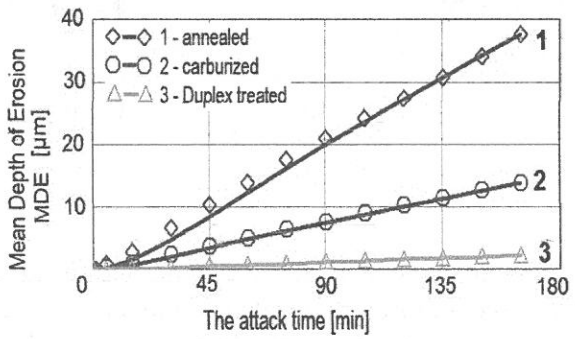

Fig.3.2. Comparisons between the variations of Mean Depth of Erosion with the attack duration, specific to the three treatment regimes

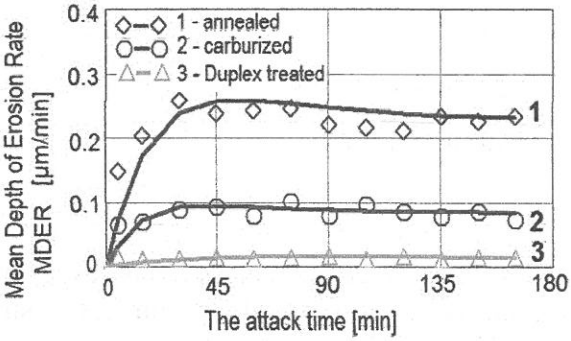

Fig.3.3. Comparisons between the variations of Mean Depth of Erosion Rate with the attack duration, specific to the three treatment regimes

From their evolutions, it can be noticed that the application of the Duplex treatment of carburization, followed by surface quenching by high frequency currents and tempering at low temperature, favors a speed reduction of the cavitation erosion of approx. 17 times compared to the annealed state and approx. 6 times compared to the carburized state.

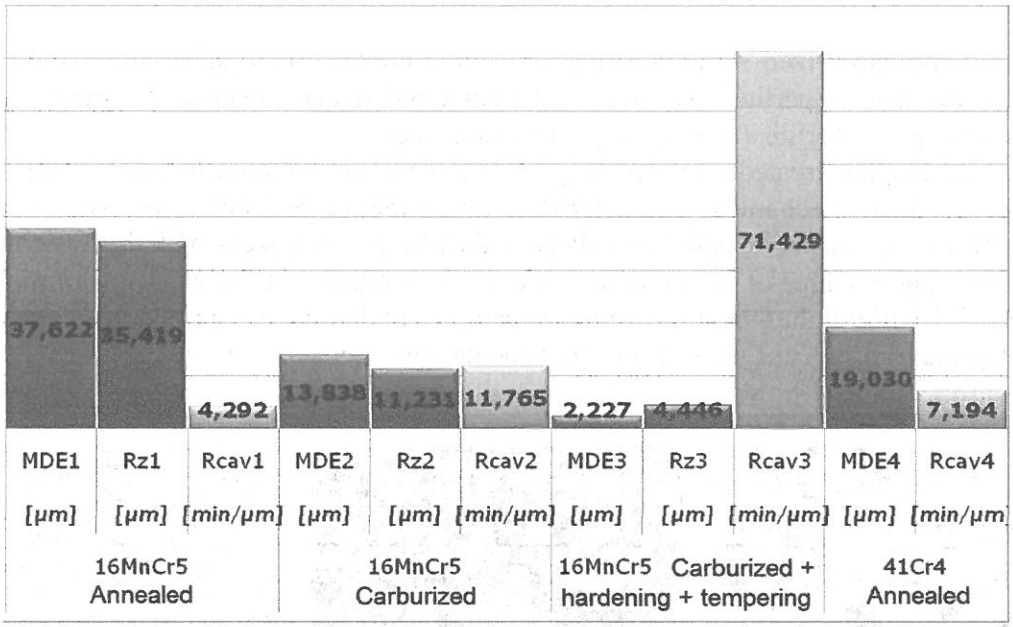

Fig.3.4. Variation of the cavitation destruction parameters depending on the applied treatment

In the histogram of Fig. 3.4 the main cavitation parameters of the samples in different treatment states are compared with those of the standard steel 41Cr4.

Thus, following the R_{cav} parameter, the highest cavitation resistance is achieved by the Duplex treatment (carburization + induction hardening + tempering): approx. 17 times greater than the one recorded for the annealed state and approx. 6 times than the one obtained for the carburized state.

Compared to the parameters of the standard steel 41Cr5, with the exception of the annealed state, which has a lower resistance (about 97% according to the MDE values and approx. 68% according to the R_{cav} values), by the carburizing and Duplex treatments, significant increases are made, as follows:

- approx. 10 times, according to the R_{cav} values and approx. 8,5 times, according the MDE values – for the Duplex treated samples;
- approx. 64 %, according to the R_{cav} values and approx. 40%, according to the MDE values – for the carburized samples.

The optical microscope investigations reveal the nature of the structural constituents associated with each stage of treatment, as follows:

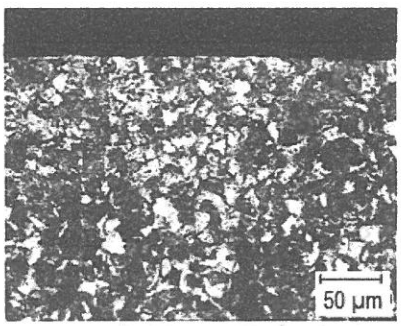

Fig.3.5. Microstrucrure of the steel 16MnCr5 in annealed state– x200

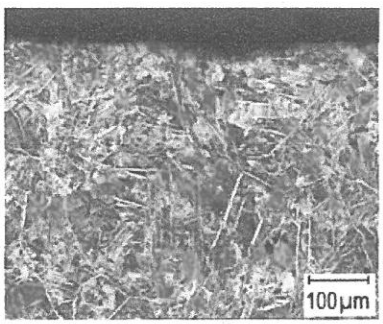

Fig.3.6. Microstructure of the carburized layer of the steel 16MnCr5 –x500

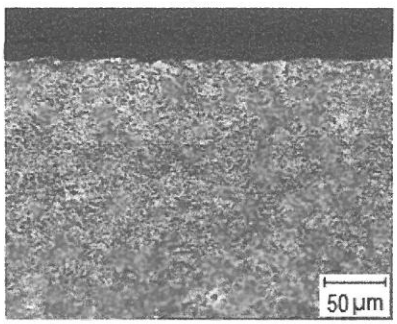

Fig.3.7. Microstructure of the Duplex treated layer –x200

- the samples in annealed state (Fig. 3.5), have the microstructure consisting of ferrite and perlite, constituents with weak mechanical characteristics and resistance to cavitation

erosion;

- at the carburized samples (Fig. 3.6), three characteristic substrates were observed, namely: outer layer – perlite + carbides (hipereutectoid steel); substrate 2 – perlite (eutectoid steel); substrate 3 – perlite + ferrite (hypoeutectoid steel);

- the Duplex treated samples (Fig. 3.7) have a predominantly martensitic structure, which gives them mechanical characteristics and superior resistance, as well as a certain amount of residual austenite and finely dispersed carbides, consistent with the basic network.

The topographies of the eroded surafaces, investigated at the electronical microscope, Fig. 3.8 – 3.10, highlight that at the annealed samples and at the carburized ones, the initiation of the degradation process starts from the proeutectoid islands, followed by the expulsion of the crystalline grains.

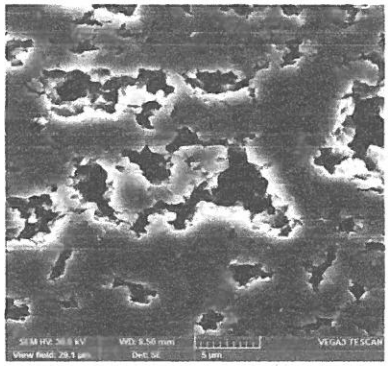

Fig.3.8. SEM image of the cavity surface of the annealed samples –x2500

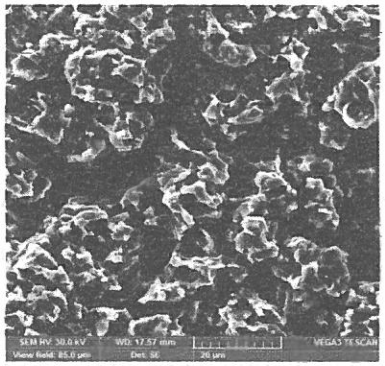

Fig.3.9. SEM image of the cavity surface of the carburized samples –x2500

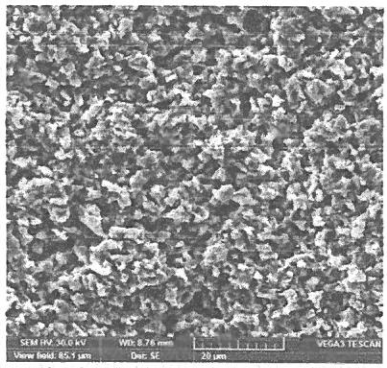

Fig.3.10. SEM image of the cavity surface of the Duplex treated samples–x2500

At the Duplex treated samples, the cracking primers are determined by both residual austenite and carbide particles, which are tough and fragile. Following the high mechanical resistance of the martensitic structure, the appearance of the cavity surface is uniform and the rupture is fragile.

The X-ray diffraction analyzes reveal the presence of ferrite, Feα in the annealed samples, at carburized sample have additionally show the iron carbide peaks Fe_3C, and at those treated with Duplex,the presence of martensite (C0.14Fe1,86) and residual austenite Feγ (Fig. 3.11).

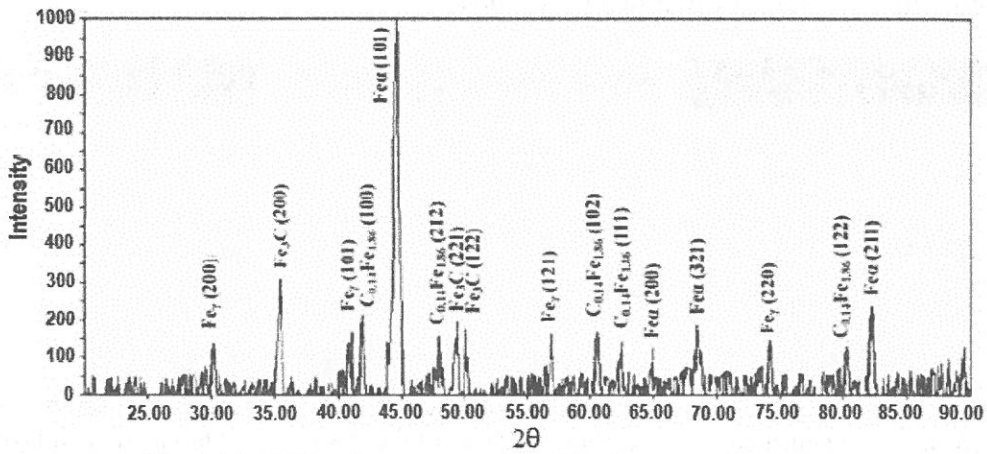

Fig.3.11. Diffraction spectra of the Duplex treated samples

The sclerometrical examinations HV0.3 made on the section of the Duplex treated layer (Fig. 3.12), indicate increased hardness values of 710 – 740 daN/mm^2 in the marginal

area, decreasing continously to the value of base material hardness, at a depth of approx. 0,9 – 1 mm.

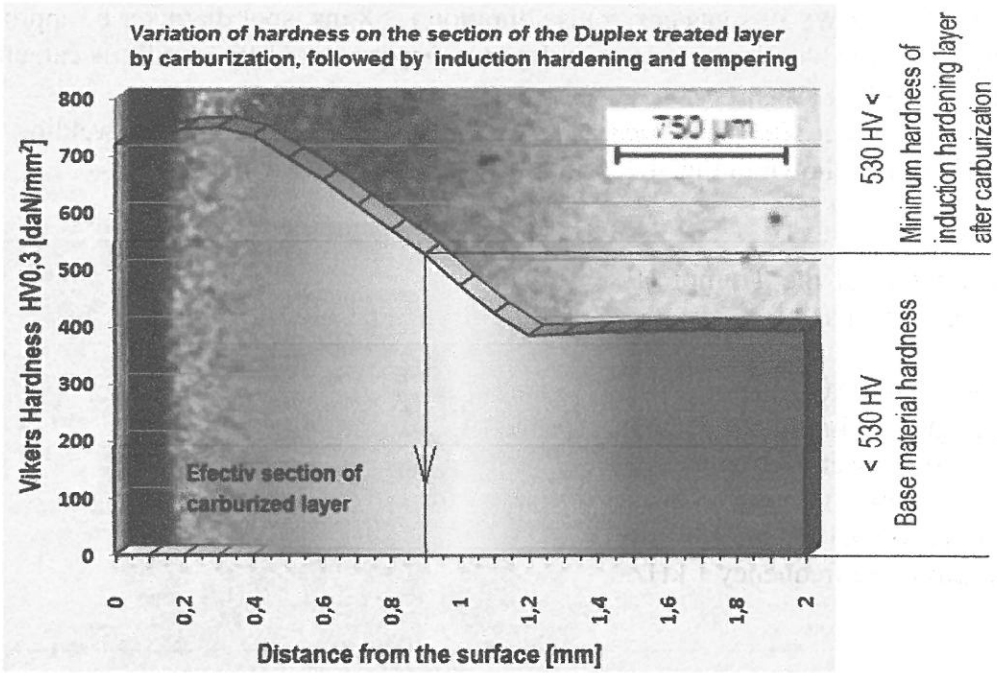

Fig.3.12. Variation of hardness on the section of the Duplex treated layer

Along with the economic effect obtained by reducing the duration of the treatment process, compared to the classic carburization followed by volumic quenching and tempering at low temperature, the analyzed Duplex treatment ensures the obtaining of a granulation, andimplicity, a martensitic structure, in the superficial layers, much finer, which justifies the significant increase of resistance to cavitation degradation.

4. The role of the annealing treatment followed by work hardening with laser beam in the increase of resistance to cavitation of the low-alloyed steel 16MnCr5

The work hardening with laser beam (known in the literature as Laser peening LP or Laser shock peening LSP) represents a hardnening process of the metallic materials surfaces, using, beneficially, the residual tensions resulted from the superficial plastic deformation of the crystalline structure of the material [10, 15], under the action of shock waves generated by the sudden variation of pressure in the formed plasma at the sample surface, at the impact of laser radiaton with a previously deposited absorbent layer.

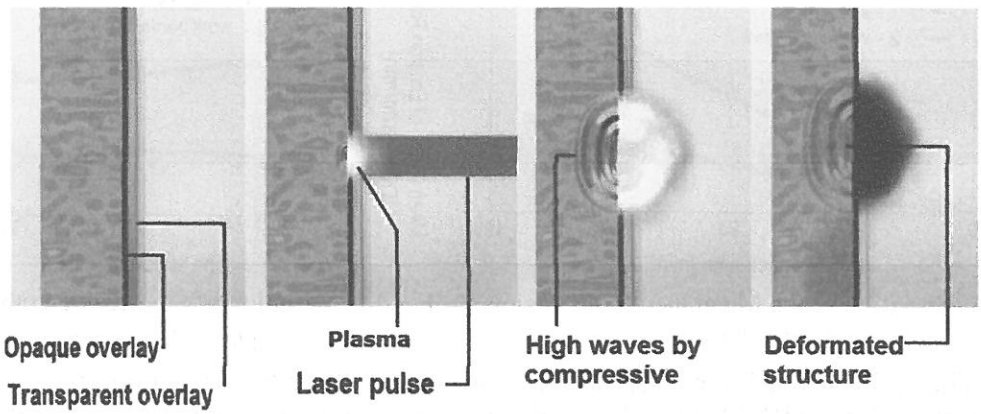

Fig.4.1. The steps of performing the laser beam ecrusion LSP

The process parameters of the ecrusion treatment are the following: pulse power of the laser beam P = 240W; 39 spots/cm^2, pulse duration t = 8 ms, spot diameter of approx. 2 mm. The energy absorbed by the opaque paint layer os approx. E = 1,92 J and it is calculated with the relation: E = P · t [W·s].

The treatment was performed at ISIM Timişoara, on a laser beam welding machine, Trumpf HL 124 P, shown in Fig. 4.2, with the parameters shown below.

The parameters of the Trumpf HL 124P laser system are:

- laser type Nd:YAG;
- wavelength 1064 nm;
- output laser power 120 W;
- maximum power in pulse 5 kW;
- pulse duration 0,3÷20 ms;
- maximum pulse frequency 1 kHz.

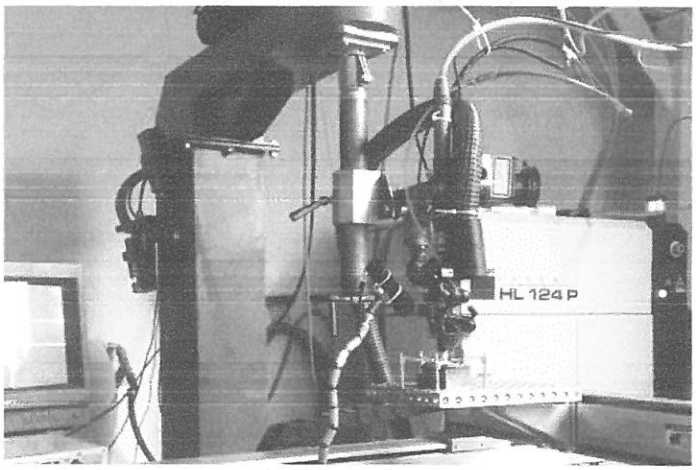

Fig.4.2. Laser micro unit, Trumpf HL 124 P

From the adjancent images, Fig. 4.3, the wavy surface is remarkable as a result of the superficial deformations, due to the impact of the laser beam.

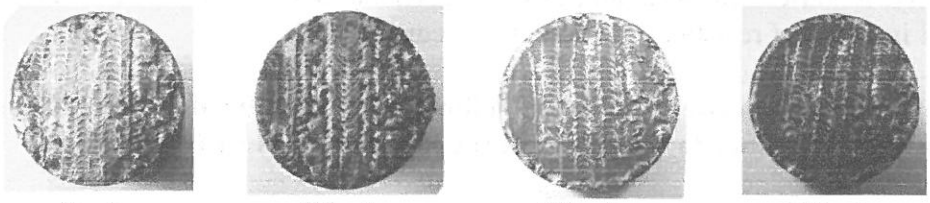

0 min 30 min 90 min 165 min

Fig.4.3. The degradation of the attack surface at different time intervals

The characteristic curves, Fig.4.4 and 4.5, show a decrease in the value of Mean Depth of Erosion Rate compared to the annealed state, and a stabilization to the maximum values, characteristic of the high hardness materials.

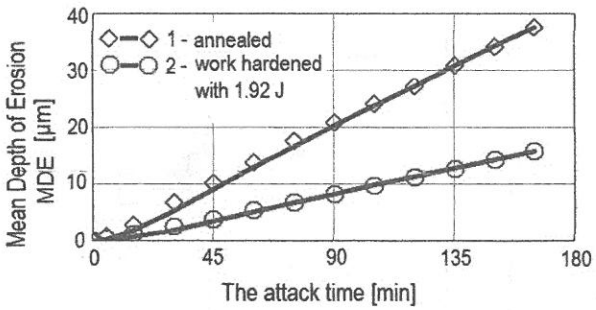

Fig.4.4. Variation of the Mean Depth of Erosion with attack time

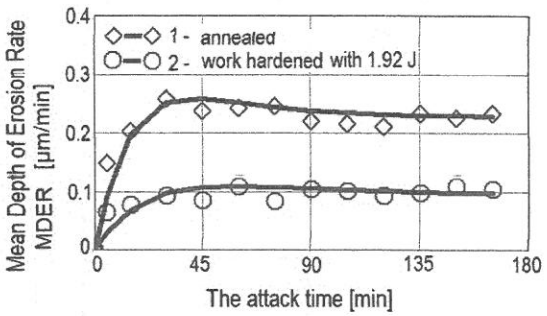

Fig.4.5. Variation of the Mean Depth of Erosion Rate with attack time

The ratio of the Mean Depth of Erosion MDE, after the 165 minutes of attack time, respectively of the $MDER_s$ speeds, of the two types of treatment, show that the ecruised

surface has a hardness of approx. 2,4 times than the one obtained by the annealing treatment.

These benefits can also be seen from the histogram shown in Fig. 4.5, in which the main characteristic parameters of cavitation resistance MDE and R_{cav} are compared, for the treatments previously described, with those of the standard steel 41Cr4.

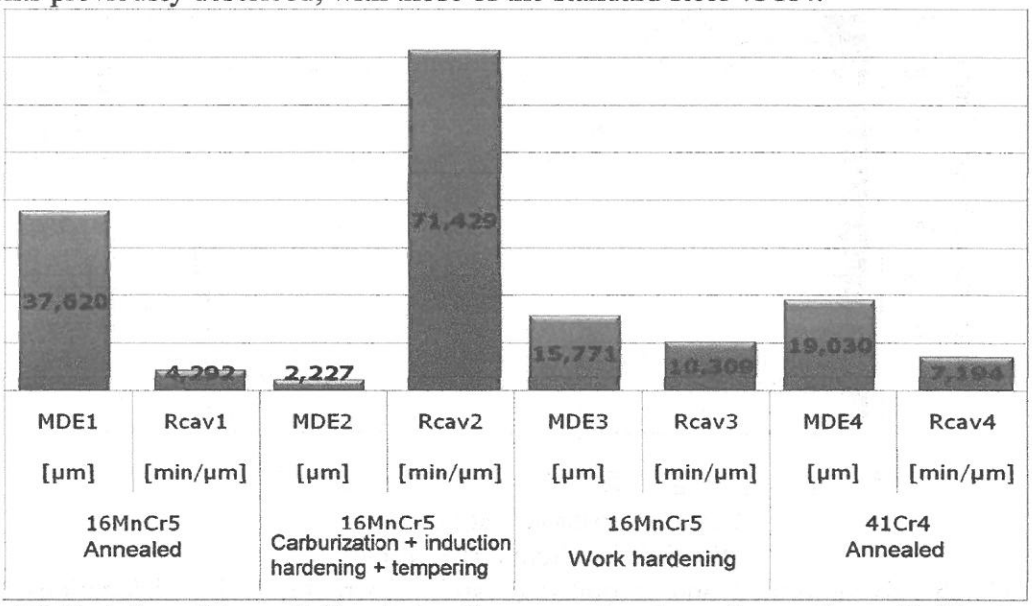

Fig.4.6. Variation of the cavitation destruction parameters depending on the applied treatment

From the analysis of the histogram shown in Fig.4.6, it is shown that by mechanical ecrusion with laser beam, the steel 16MnCr5 benefits of an increase of cavitation resistance of approx. 2,4 times compared to the annealed state, respectively with approx. 43% compared to the standard steel 41Cr4. We appreciate that this gain is caused by the increase in the hardness of the ecruised layer.

From the microscopic images, Fig.4.7 and 4.8, the following are remarked, the accentuated degradation of the annealed state, the presence of the deformed structure at the surface of the material, and the fact that the work hardened layer was not overcome after the cavitational tests.

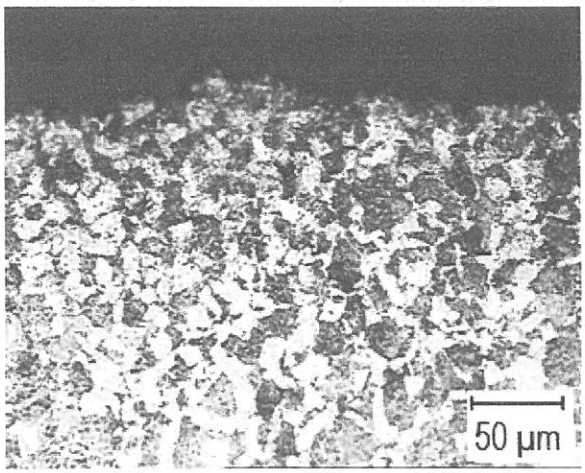

Fig.4.7. Microstructure of the steel 16MnCr5 in annealed – x 200

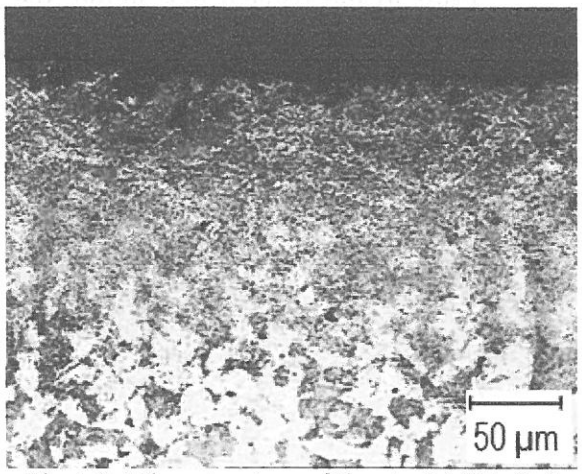

Fig.4.8. Microstructure of the steel 16MnCr5 superficially work hardened with laser beam – x 200

The hardness measurements on the section of the hardnened layer (Fig. 4.9), indicates increases of the values in the marginal area of up to 590 – 597 daN/mm^2, which gradually

decrease to the value of the core hardness, at a depth of approx. 0,2 mm.

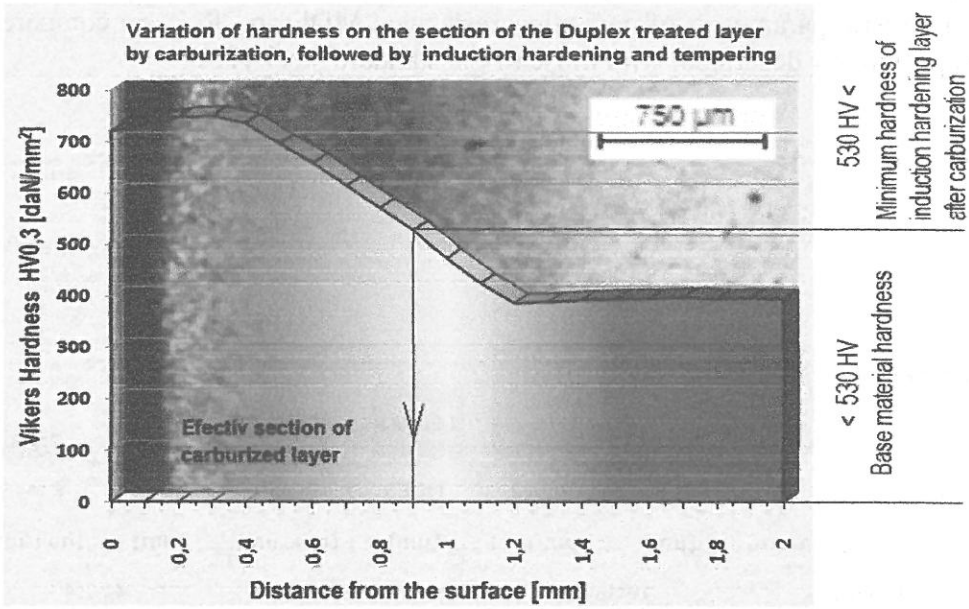

Fig.4.9. Gradient curve of hardness

The highly deformed and saturated crystalline structure with dislocations, resulted from the work hardening with laser beam treatment, is characterized by a degree of fragmentation and high finishing, which favors the increase of hardness and the other mechanical characteristics, while increasing the resistance to cavitation erosion.

5. Thermal quenching and tempering treatment followed by gas nitriding and their influence on the cavitation erosion of the alloy steel 34CrNiMo6

Another method of increasing the cavitation erosion resistance, applied to the alloy steel 34CrNiMo6, is the Duplex treatment by quenching and tempering [15, 17], followed by the thermochemical treatment of nitriding by two technologies, namely nitration in the gaseous environment and with the laser beam.

Prior to mechanical machining, the material was undergone an thermal treatment of annealing, followed by a thermal treatment by hardening and tempering, according to the cyclogram in Fig. 5.1.

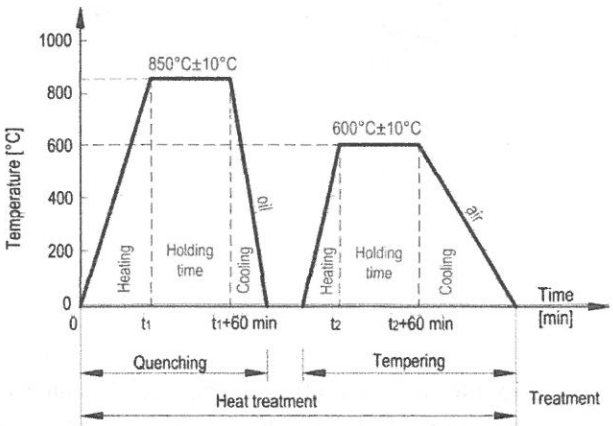

Fig.5.1. Hardening and tempering thermal cyclogram

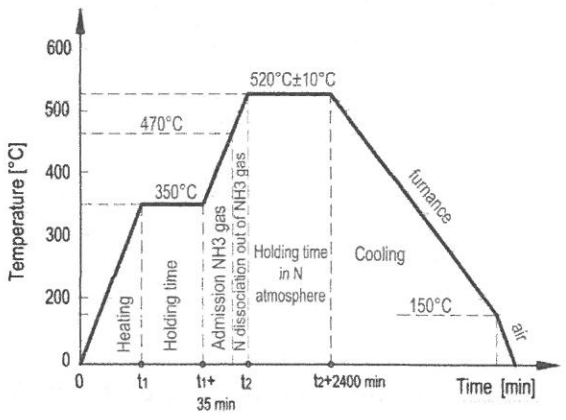

Fig.5.2. Nitriding thermal cyclogram

Subsequently to the mechanical machining and rectification of the final quotas, some of the samples were subjected to a thermochemical treatment of gas nitriding, according to the

cyclogram of Fig. 5.2, after which in the superficial layer, simple and complex nitrides formed, dispersed in a solid solution rich in Nitrogen [15], which prevents the displacements of atoms along the sliding planes of the crystalline network and implicitly, the increase of the mechanical characteristics, especially of the hardness.

From the characteristic cavitation curves, Fig. 5.3 and 5.4, after the 165 minutes of attack, it is observed that the values of the nitrited samples, are much lower compared to the annealed and improved state, which means an increased resistance to cavitation erosion.

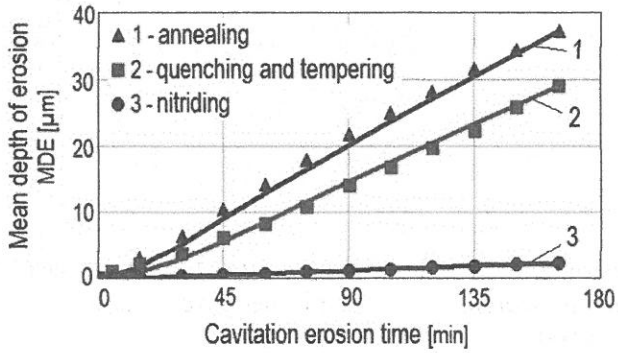

Fig.5.3. Variation of the Mean Depth of Erosion with attack time

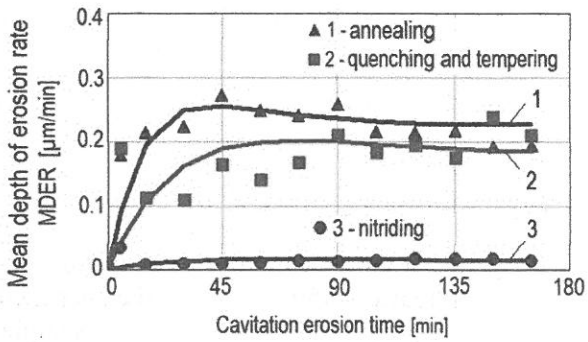

Fig.5.4. Variation of the Mean Depth of Erosion Rate with attack time

In orded to highlight the benefits of the performed treatments on the increase of the resistance to cavitation erosion of the steel 34CrNiMo6, as well as it's annealed state, in the histogram of Fig. 5.5, the Mean Depth Erosion MDE values are compared, determined after 165 minutes and the cavitation resistance parameter with the afferent values to the standard steel 41Cr4 (also in the annealed state).

It is noticeable that in the annealed state, the cavitation resistance increases by approx. 23 % after the quenching and tempering treatment, respectively approx. 15,7 after the gaseous nitriding treatment.

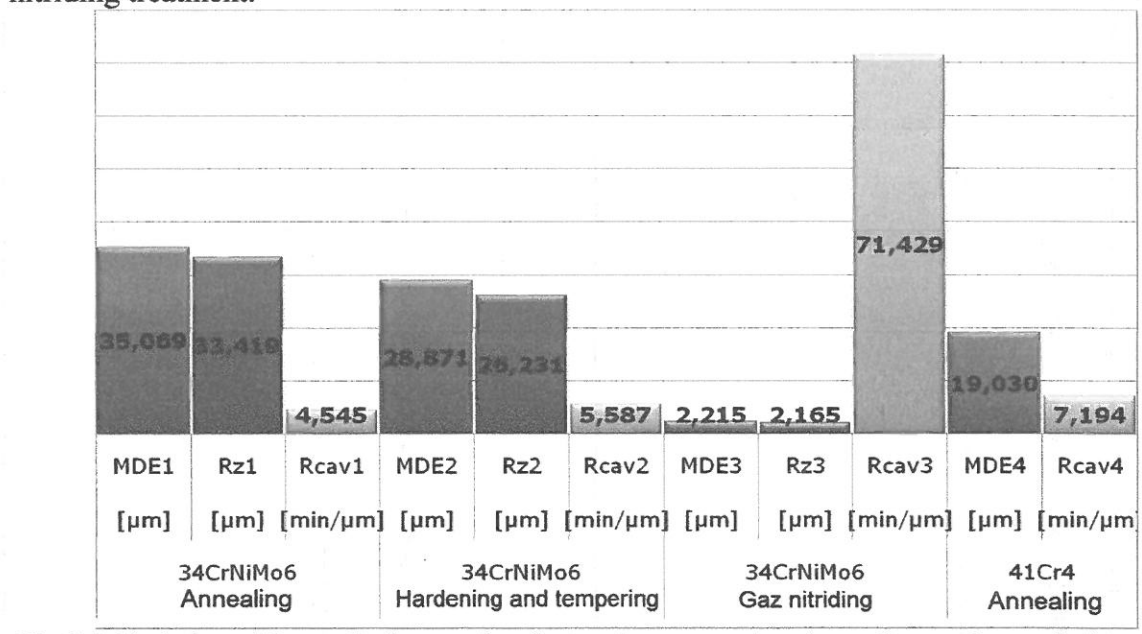

Fig.5.5. Variation of the cavitation erosion destruction parameters depending on the applied treatment

The approximate values of the cavitational parameters, the calculated Mean Depth of Erosion MDE and roughness R_z measured at the end of the cavitation test, certify the correctness of determinations.

The microstructural investigations, Fig. 5.6 – 5.8, show that the structure of the

annealed material is made of proeutectoid ferrite and bainite [14, 15], after the improvement a sorbitical tempering structure results, made of acicular ferrite and globular carbides [14, 15], which provides the best ratio between resistance, ductility and tenacity.

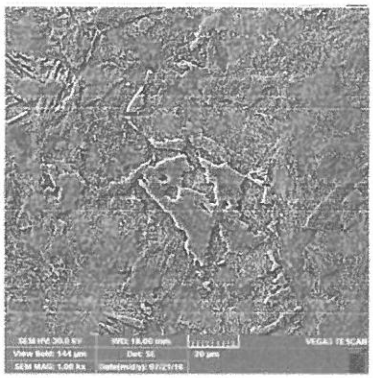

Fig.5.6. Microstructure of annealed – x500

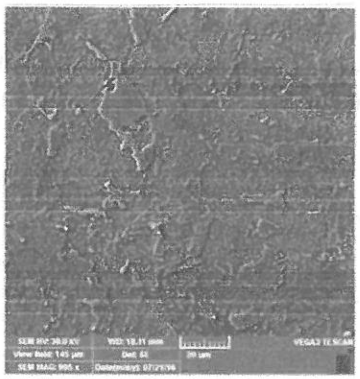

Fig.5.6. Microstructure of the quenched and tempered samples – x500

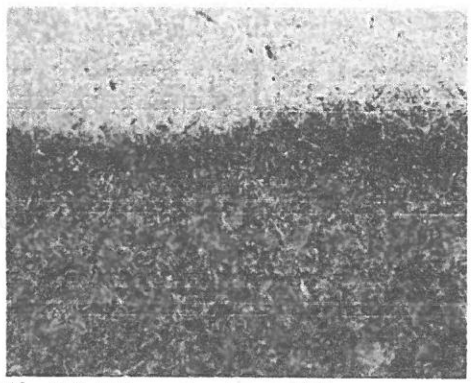

Fig.5.8. Microstructure of the gaseous nitrided layer – x500

At the nitrided samples, the presence of the nitrides in the superficial layer can be noticed, which gives it a significant increase in hardness [15].

As a result of indexing, it is noted that the annealed and improved samples (Fig. 5.9), contain, in addition to iron, the same alloying elements, varying their proportions depending on the nature of the structural constituents present in the investigated area.

At thenitrided samples (Fig. 5.10), in addition to the elements present in the base material, the presence of nitrogen in the surface layers is found, in a significant content.

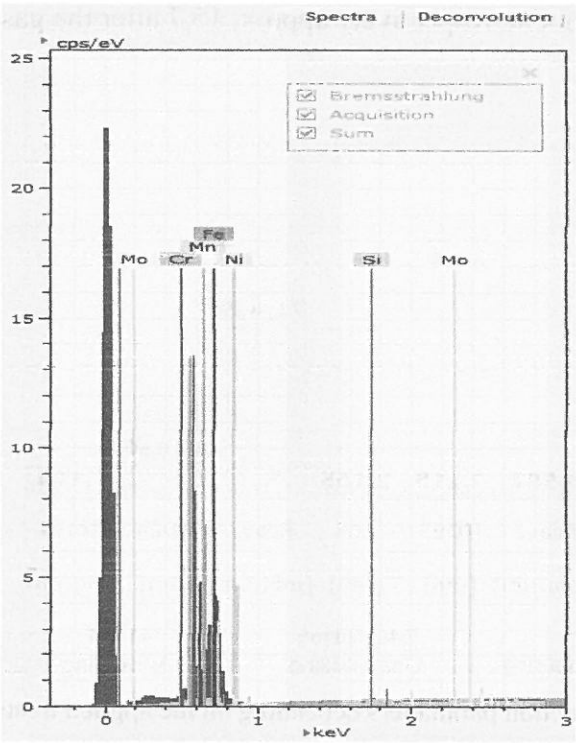

Fig.5.9. Dispersion spectra of the quenched and tempered samples

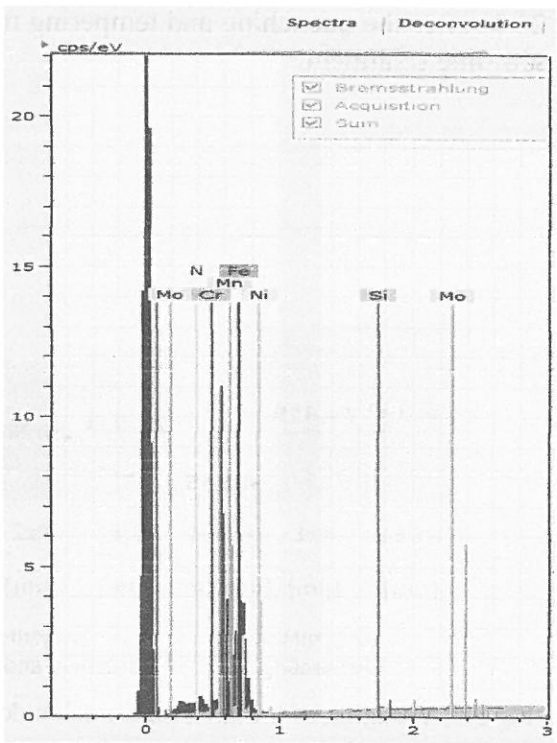

Fig.5.10. Dispersion spectra of the nitrided sample

The diffraction analysis of the samples, reveals only the presence of ferrite in the annealed and quenched and tempered steel structure (Fig. 5.11.a), respectively the presence

of nitrides type Fe_3N, Fe_4N, in the structure of the Duplex treated material (Fig. 5.11.b), confirms that the nitriding treatment was carried out properly.

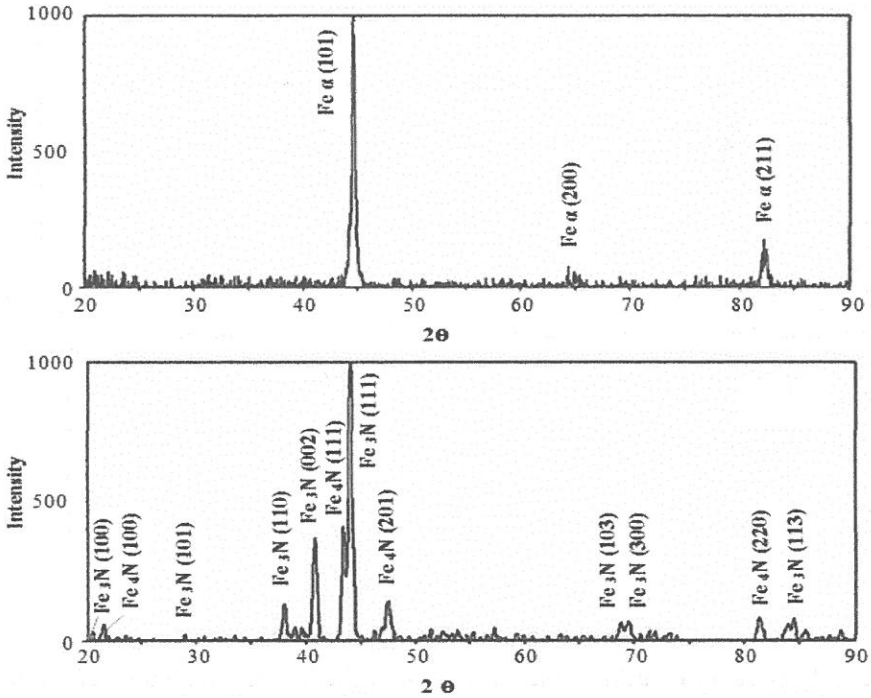

Fig.5.11. X-ray diffraction: a – samples in annealed and quenched and tempered state, b – gas nitrided samples

The topographies of the cavitated surfaces, fig. 5.12 – 5.14, highlight the fact that at the annealed samples, the intensity of the degradation phenomenon of the surface is maximal, the proeutectoid ferrite islands being prefferentially attacked by microcracking followed by the epulsion of the crystalline grains [3]. A similarly qualitative situation also occurs at the improved samples, in the sense that the crack initiation also occurs in the ferrite areas, soft and plastic constituent, with weak mechanical resistance.

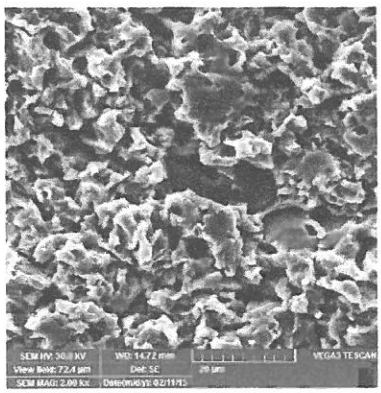

Fig.5.12. SEM image of the annealed and cavitated sample surface – x2000

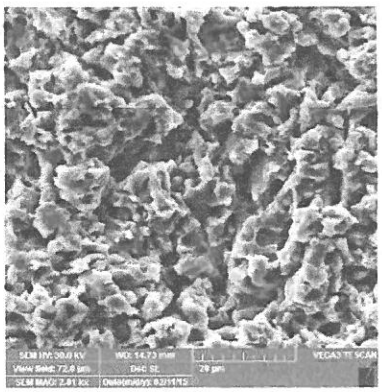

Fig.5.13. SEM image of the i quenched and tempered and cavitated sample surface – x2000

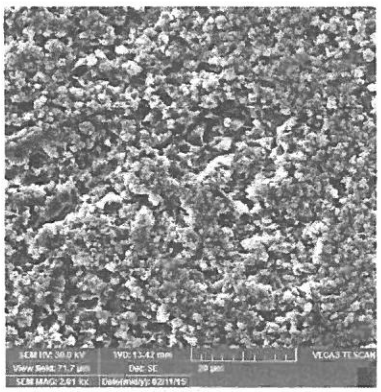

Fig.5.14. SEM image of the nitrided and cavitated sample surface – x2000

At the Duplex treated samples, the cracking primers are determined by the nitride particles and by the separation limits between them, as well as by the separation limits between the nitrogen ferrite grains. The microstructure with high hardness of the marginal layer causes a small and uniform wear, with fine pinching, without the appearance deep craters.

The hardness measurements of the depth of the nitrided layerindicates increases in its values in the marginal area of up to approx. 870 daN/mm^2, which will gradually decrease towards the inside of the piece, at a depth of 0,38 mm.

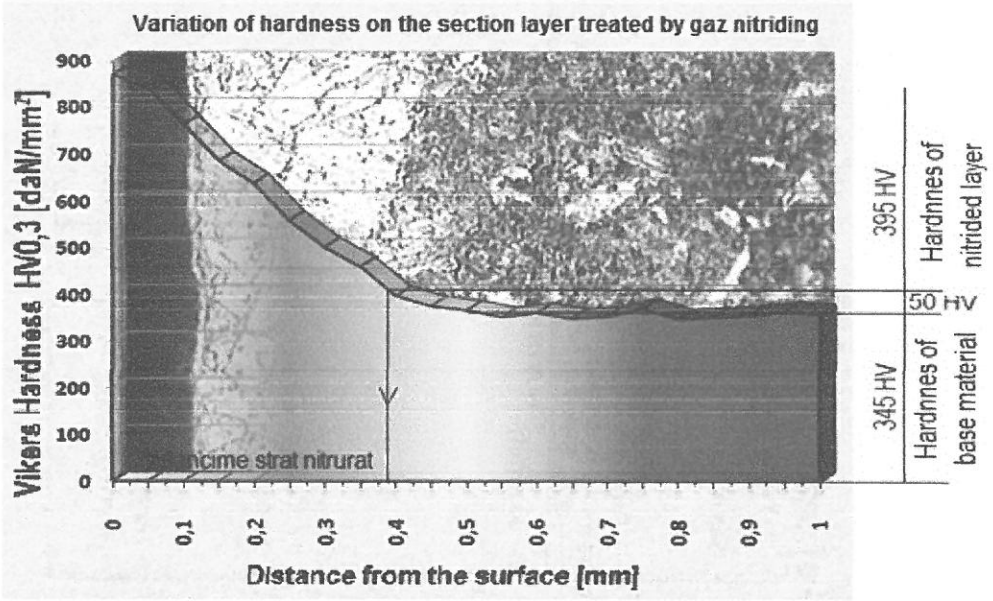

Fig.5.24. Variation of hardness on the section of the Duplex treated by gas nitriding layer

Although the nitriding treatment implies addictional high costs, it is fully justified due to the prolongation of the lifetime of the hydraulic equipment components, which work in cavitation conditions, the reduction of maintenance times and costs during the exploitation period.

6. Thermal quenching and tempering treatment followed by nitriding with laser beam and their influence on the cavitation resistance of the alloyed steel 34CrNiMo6

The second laser beam nitriding process [6, 7, 13, 15], was carried out on the same Trumpf HL 124 apparatus, and consists of bombarding the surface with a pulsed laser beam at three pulse power regimes, namely 240 W, 180 W, 120 W, in a pure nitrogen environment. Under the action of the laser beam, the superficial metal layer melted at a certain depth, allowing the accelerated diffusion of nitrogen into the melting mass and the formation of nitrides by alloying with Fe and other alloying elements [6, 13, 15]. The images show the wavy appearance of the surfaces resulting from the impact with the laser beam.

Nitrided sample with laser beam at P = 120 W

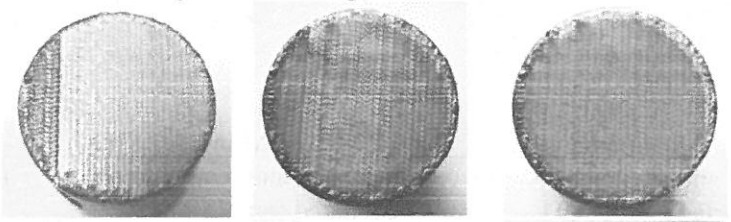

Nitrided sample with laser beam at P = 180 W

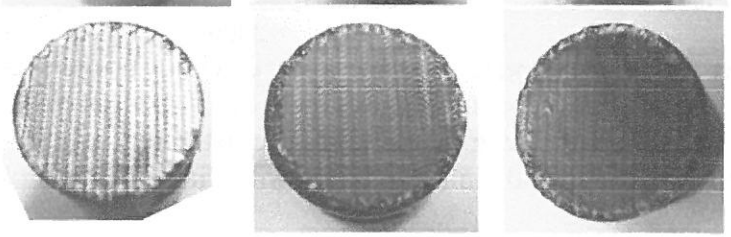

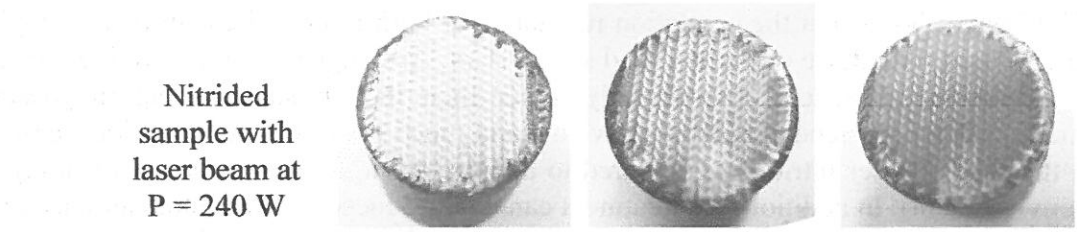

Fig.6.2. Surfaces treated by nitriding with laser beam at three power regimes, subjected to cavitation, at different time intervals

The characteristic curves, MDE(t), MDER(t) show that by nitriding with laser beam, a substantial increase of the cavitation resistance realises, compared to the improved samples, proportional to the beam power.

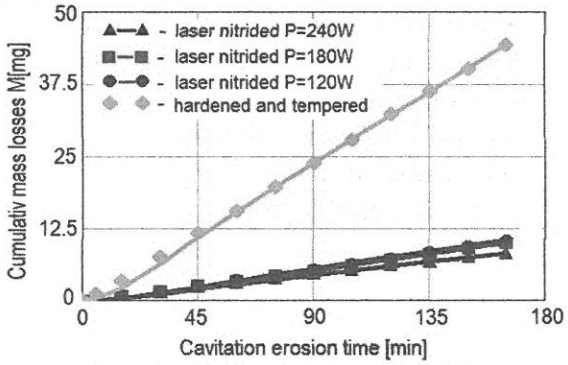

Fig.6.2. Variation of the Mean Depth of Erosion with attack time

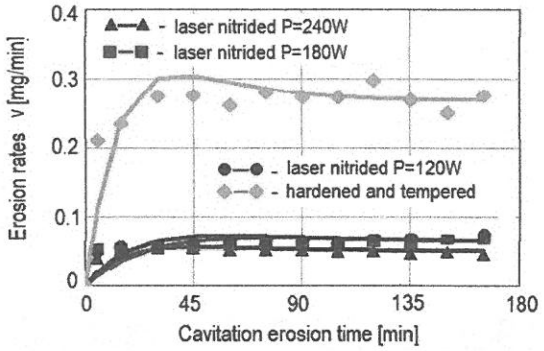

Fig.6.3. Variation of the Mean Depth of Erosion Rate with attack time

Out of the three laser nitriding regimes, the highest resistance is given by the one realized at a power of P = 240 W.

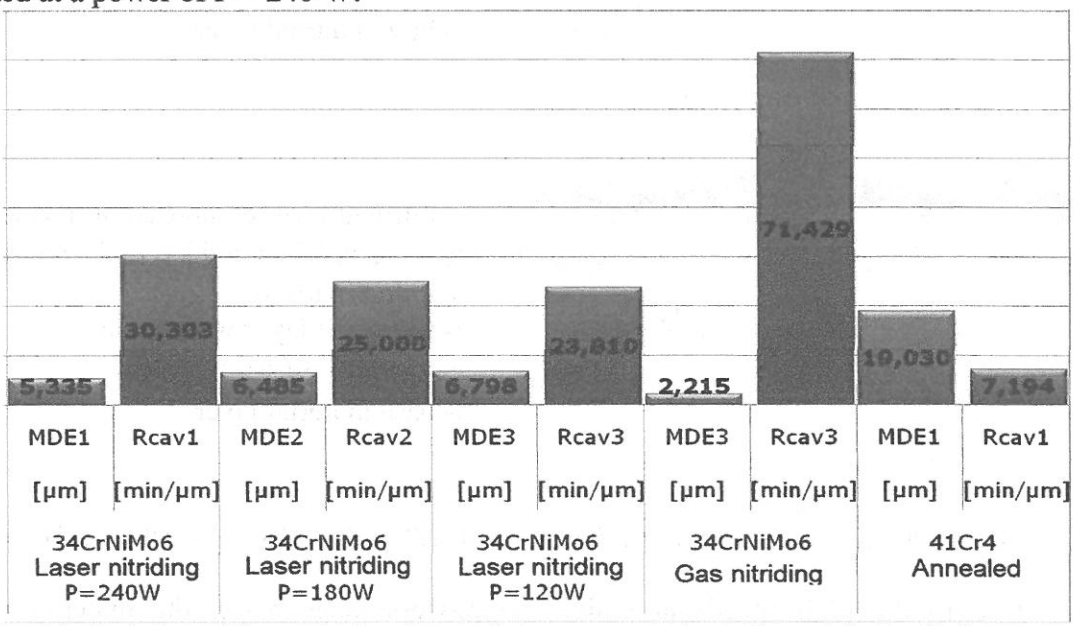

Fig.6.4. Variation of the cavitation destruction parameters depending on the applied treatment

In the histogram of Fig. 6.4, the comparison of the main cavitational parameters is realized, recommended by ASTM G32-2010 normatives and are used in our cavitation laboratory, for all gas nitriding procedures, with those of the reference steel 41Cr4, in annealed state.

The image shows that the cavitation resistance of both laser and gas nitrided samples have higher values then those of the standard steel 41Cr4. Although the laser nitriding process leads to cavitation resistances, substantially lower then the classic nitriding in gaseous environment, it is recommended due to a low cost and much lower treatment period (approx. 3 min in the case of laser nitriding, compared to approx. 40 hours in the case of nitriding in gaseous environment). In addition, the treatment can be introduced into an automation cycle.

From the microscopic images it is observed that all three regimes have a melt zone, consisting of nitrides type ε si γ' embedded in the solid solution matrix α, followed by a bainito-martensitic structure transmision area, adjacent to the melted layer, formed due to the self-quenching of the material at relatively low critical speeds [15].

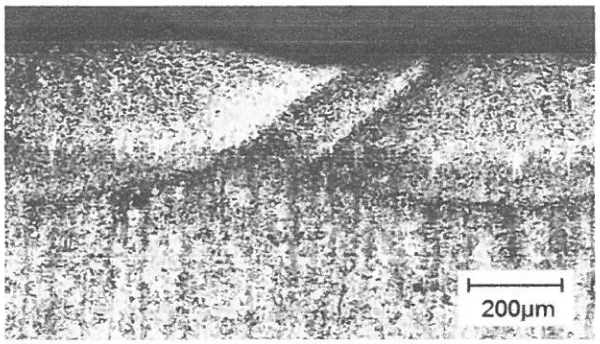

-a-

‹- nitrided layer composed of nitrides type ε , andγ' embedded in the solid solution matrixα;
‹- transition layer with bainito-martensitic structure;
‹- base material layer.

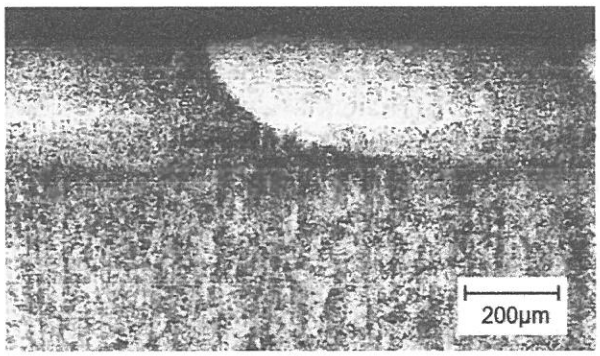

-b-

‹- nitrided layer composed of nitrides type ε , andγ' embedded in the solid solution matrixα;
‹- transition layer with bainito-martensitic structure;
‹- base material layer.

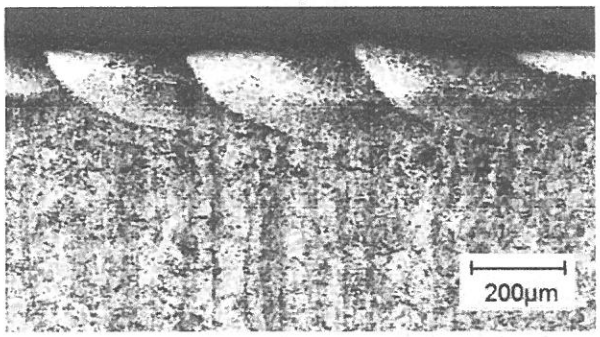

-c-

‹- nitrided layer composed of nitrides type ε , andγ' embedded in the solid solution matrixα;
‹- transition layer with bainito-martensitic structure;
‹- base material layer.

Fig.6.5. Section through the laser beam nitrided layer at: a)P = 240W, b) la P =180 W, c) la P=120 W,

Due to the high speeds at which the process takes place, the material remains unaffected after the passage area.

The hardness gradient curve, Fig. 6.6, indicates increases at values of 790 – 810 daN/mm^2 in marginal area, gradually decreasing to the value of the base material, at a depth of approx. 0,67 mm.

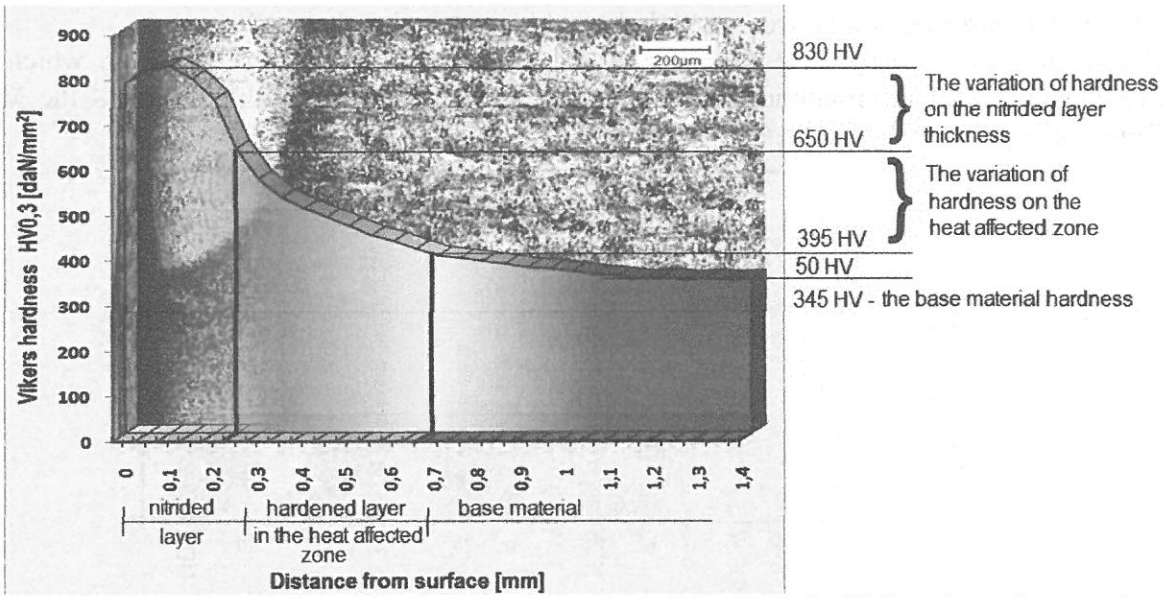

Fig.6.16. Variation of hardness on the section of the nitrided with laser beam layer at the power P=180 W.

7. The proposal of the R_z roughness parameter in the evaluation of the resistance to cavitation of the materials

The conclusion obtained by the team of the cavitation laboratory, of the Polytechnic University of Timişoara, after countless attempts, on a lot of materials, led to the idea that there is a dependence between the MDE parameter (recommended by the ASTM G32-2010 normatives) and the measured R_z material roughness, which can allow the use of R_z in the evaluation of the behavior, respectively the resistance of the material to the cavitation erosion. So, due to the large number of measurements (270), three materials from different categories were chosen on which the roughness measurements were made, namely:

- alloyed steel 16MnCr5 – in the annealed state and carburized, researched in this thesis;
- bronze AMPCO M45 subjected to the thermal quenching treatment [18];
- alloyed steel 42CrMo4 – in annealed state, also used the manufacturing of hydraulic components.

For each sample, the cavitate surface was divided in 9 square areas, according to Fig. 7.1, on which the roughness parameters were measured in two perpedicular directions (18 measurements in total).

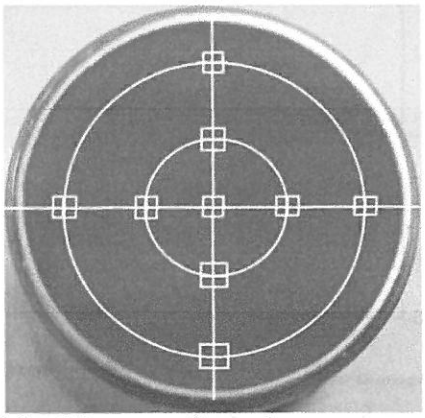

Fig.7.1. Scheme of the 18 areas of roughness parameters R_a, R_z and R_t

The values of the R_z, at different test intervals (i.e. 0, 30, 75, 120 and 165 minutes) in

all the 18 measuring points, were recorded in tables, averaging their values.
Based on these measurements, the histograms of Fig. 7.2 – 7.4 were made, in which the average values of the roughness parameter, R_z, are compared with the values of the Mean Depth of Erosion, calculated as the mean of the three tested samples.

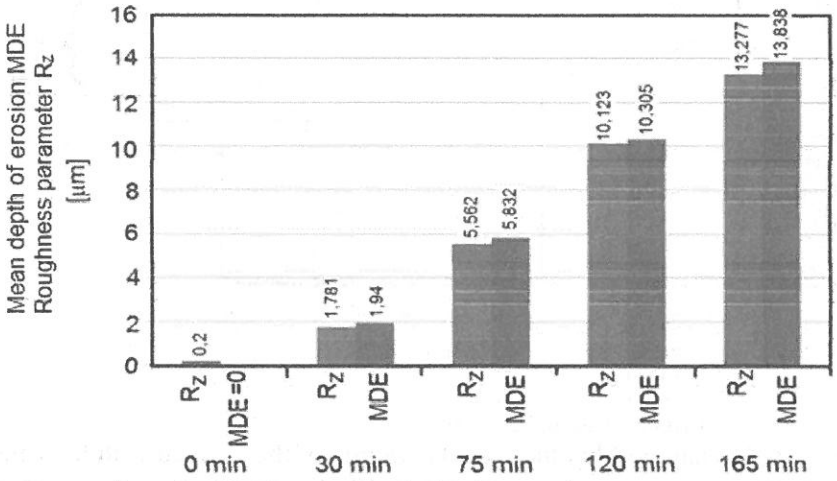

Fig.7.2. Comparison the MDE parameter with the roughness parameter R_z (steel 16MnCr5 – annealed state and carburized)

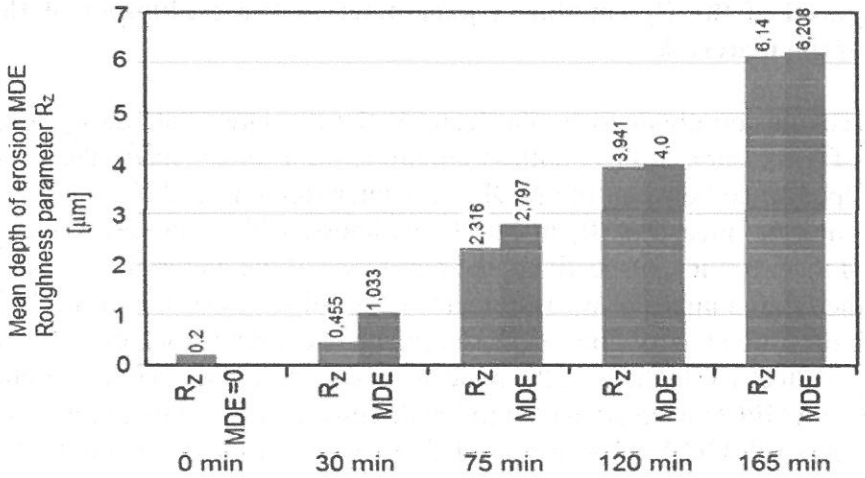

Fig.7.3. Comparison the MDE parameter with the roughness parameter R_z (AMPCO M45 bronze – quenching and tempering)

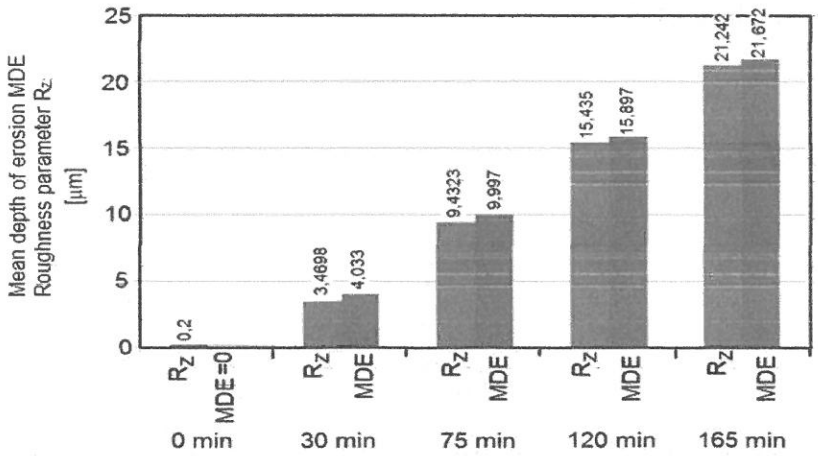

Fig.7.4. Comparison the MDE parameter with the roughness parameter R_z (steel 42CrMo4 – annealed state)

In the histograms from the adjacent figures, the average values of the R_z roughness are compared with the values of the Mean Depth of Erosion MDE, calculated as the mean of the three tested samples, from which it is found that, regardless of the duration we refer to, the values of the parameter R_z is poorly inferior to the value of the MDE parameter (which is affected by the removal of dust and asperities from the first minutes of attack).

It is also noted that as the cavitation duration increases, the difference between MDE and R_z become smaller, due to the hardening of the superficial layer, unde the mechanical impact of the microjets and shock waves.

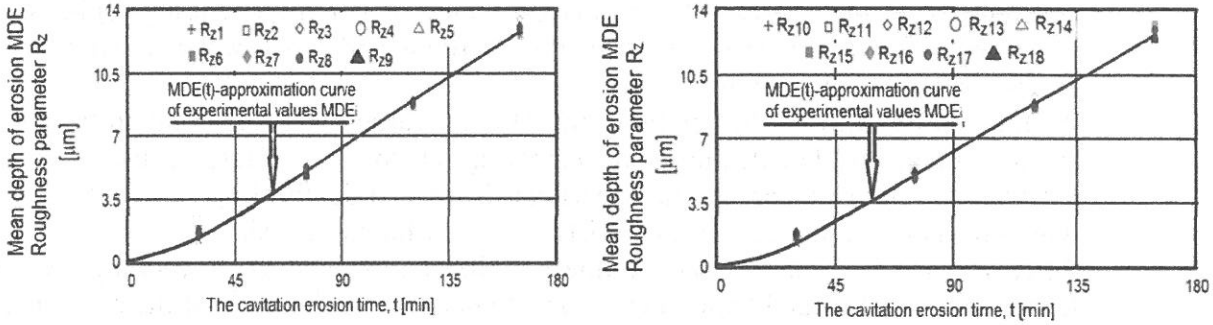

-a- -b-

Fig.7.5. Dispersion of the R_z parameter towards the approximation curve of the Mean Depth of Erosion values, steel 16MnCr5 annealed and carburized: a) R_z values from 1 to 9; b) R_z values from 10 to 18

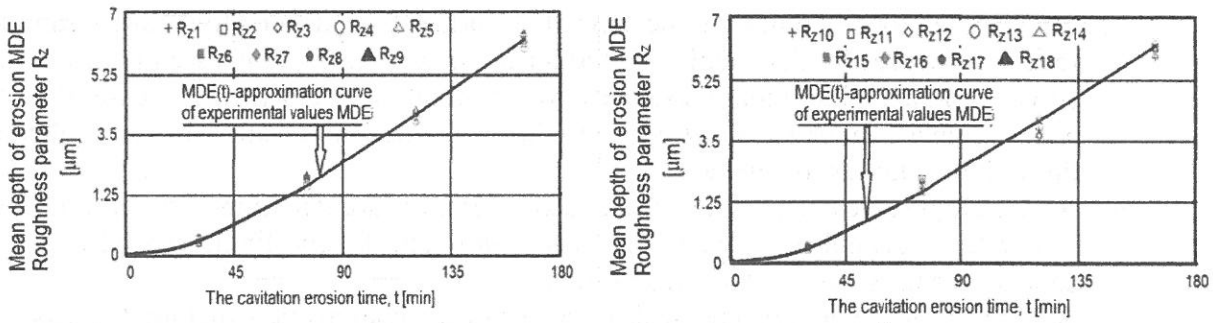

-a- -b-

Fig.7.6. Dispersion of the R_z parameter towards the approximation curve of the Mean Depth of Erosion values, AMPCO45-TT bronze: a) R_z values from 1 to 9; b) R_z values from 10 to 18

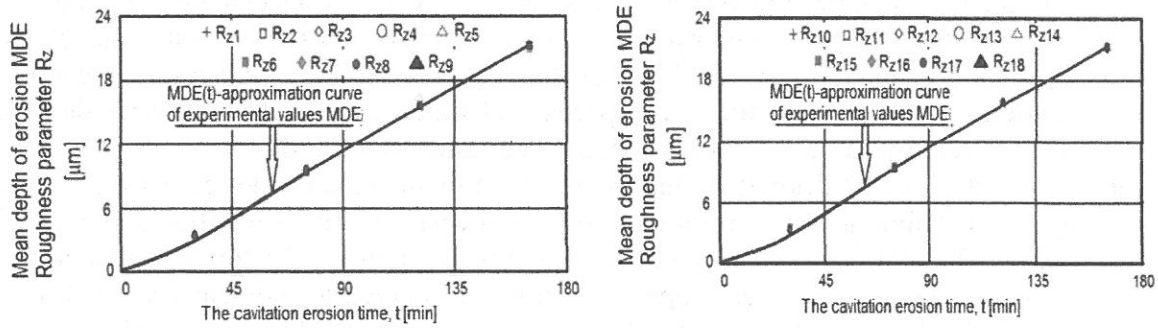

-a- -b-

Fig.7.7. Dispersion of the R_z parameter towards the approximation curve of the Mean Depth of Erosion values, steel 42CrMo4 annealed: a) R_z values from 1 to 9; b) R_z values from 10 to 18

In the diagrams of Fig. 7.5...7.7, the disperson of the R_z parameter values are presented towards the mediation curves, constructed with the statistical relations, for each material. It is found that these dispersions are very low, similar to the MDE_i experimental values, obtained for the three samples, which certifies the correctness of the method. Therefore, the parameter R_z represents a very good evaluation of the material degradation to cavitation erosion.

CAP 8. Final conclusions and original contributions. New research directions.

Final conclusions and original contributions

1. The deepening of studies regarding the causes which determines the cavitation in the hydraulic drive systems, especially in the control, distribution and adjustment devices, and finding solutions to ensure a good dynamic operation is a necessity, both in terms of safety in operation and economical point of view, the hydraulic equipment was completely replaced due to the deterioration.
2. The researched materials are intended for the manufacture of mobile parts in hydraulic, control and regulations devices, which, under the operating regimes, are subjected to the destrucxtive attack of the microjets and shock waves created by the cavitation bubble implosion.
3. At the steel 16MnCr5, by applying the Duplex carburizing treatment, followed by surface induction haerdening and tempering at low temperature, favors a fine martensitic microstructure in the superficial layer at a depth of approx. 0,9 – 1 mm, which results in an increase of the resistance to cavitation degradation.
4. After the Duplex carburizing treatment, followed by surface quenching by high frequency induction and tempering at low temperature, an increase of the resistance to cavitation erosion is obtained, of approx. 17 times higher compared to the annealed state, respectively of approx. 10 times compared to the standard steel 41Cr5, thus contribuiting to the increase of the life spanof the device under intensive cavitation conditions.
5. The typical topographies of the cavitated surfaces, at differently treated samples, reveal a preferential degradation of the ferrite areas, a fost and plastic microstructural constituent, a slightly higher resistance to the initiation of cracks in the case of perlite and a maximum crack resistance provided by the martensitic structure obtained through the Duplex treatment.
6. At the Duplex treated samples, the cracking primers are determined by both residual austenite, structural constituent with a low flow and fatigue limit, as well as by the carbide particles that are though and fragile.
7. As a result of the high mechanical resistance of the martensitic structure, the aspect of the cavitated surface is uniform and the rupture has a fragile character.
8. The work hardnening treatment using laser beam, leads to a highly deformed and saturated crystalline structure with dislocations, with an accentuated fragmentation and finishing degree, favoring the increase of hardness and other mechanical resistance characteristics. Such a structural state justifies a reduction of cavitation erosion of the steel 16MnCr5 of approx. 2,4 times compared to the annealed state, respectively by approx. 43% compared to the standard steel 41Cr5.
9. At the steel 34CrNiMo6, the Duplex treatment by quenching and tempering, followed by gas nitriding, although it implies additional costs, it is fully justified due to the fact that it offers the highest resistance to cavitation of approx. 17,5 times compared to the annealed state, respectively approx. 10 times compared to the standard steel 41Cr4, due to nitrides formed in the superficial layer, characterized by a high hardness.
10. The technological variant of the laser beam nitriding, favors an increase of the cavitation erosion resistance of approx. 3,3...4,2 times compared to the annealed state of the standard steel 41Cr4.
11. The increase of the laser beam power is manifested by an increase in the depth of melted layer, and with the increase of the solidification and cooling time of the melted mass in the nitrogen environment, there is implicitly an increase in the duration of the

nitrogen diffusion in the superficial layers. These phenomena justifies the improvement of the resistance to cavitation erosion.

12. The roughness parameter R_z can be used at the evaluation of the destruction degree by cavitation, being roughly equal to the Mean Depth of Erosion MDE, recommended by the ASTM normatives. The advantage of using R_z is that its value is closer to reality, being obtained by measurements.

New research directions

Starting form the carried out researches, within this doctoral program, the following perspectives can be formulated in terms of the results obtained and presented in the paper:

- opportunities to improve the resistance to cavitation of the steels intended for the construction of hydraulic systems by using materials other than those researched in this paper;
- widening of the Duplex treatments database, through new combinations of treatments that can be applied to steels used in the manufacture of hydraulic system equipment in order to increase the reliability and safety in exploitation;
- development of new concepts for the evaluation of the resistance to cavitation erosion;
- creation of hierarchy classes after the resistance to vibratory cavitation using as a criterion the values of the roughness parameter R_z.

BIBLIOGRAPHY (SELECTION)

[1] Anton I.: „Cavitaţia", vol. I, Editura Academiei RSR, Bucureşti, 1984
[2] Anton I.: „ Cavitaţia", vol. II, Editura Academiei RSR, Bucureşti, 1985
[3] Bordeaşu I.: „Eroziunea cavitaţională a materialelor", Editura Politehnica, Timişoara, 2006
[4] BordeaşuI., PopoviciM.O., **Ghera C.**, SălcianuL.C., MicuL.M., PodoleanuC.E., „Cavitation erosion behavior of the steel 17CrNiMo6", Machine design, vol. 8, nr. 4, Ungaria, pp. 149-154, 2016
[5] Bordeaşu I., Popoviciu M.O., Sălcianu L.C., **Ghera C.**, Micu L.M., Bădărău R., Iosif A., Pirvulescu L.D., Podoleanu C.E.: „A new concept for stainless steels ranking upon the resistance to cavitation erosion", International Conference on Applied Science, vol. 163, 2017
[6] Czerwinski F., „Thermochemical Treatment of Metals", CanmetMATERIALS, Natural Resources Canada, Hamilton, Ontario, Canada, 2012
[7] Da SilvaF.J.,a.o.,„Cavitation erosion behavior of ion – nitrided 34CrAlNi7 steel with different microstructures", Wear, Vol.304, Iss.1-2, pp. 183 – 190, 2013
[8] Franc J.P., et al., „La cavitation. Mécanismes physiques et aspects industriels", Press Universitaires de Grenoble, Grenoble, France, 1995
[9] Garcia R., Hammitt F.G., Nystrom R.E., „Correlation of cavitation damage with other material and fluid properties, Erosion by Cavitation or Impingement", ASTM, STP 408 Atlantic City, New Jersey, U.S.A., 1960
[10] **Ghera C.**, MiteleaI., BordeasuI., CrăciunescuC.M., „Improvement of cavitation erosion resistance of a low alloyed steel 16MnCr5 through work hardening", METAL 2015 - 24th International Conference on Metallurgy and Materials, Brno, Cehia, pp. 661-666, 2015
[11] **Ghera C.**, Mitelea I., Bordeasu I., Crăciunescu C.M., „Effect of Heat Treatment on the Surfaces Topography Tested at the Cavitation Erosion from Steel 16MnCr5", Advanced Materials Research, vol. 1111, pp. 85-90, July 2015
[12] **Ghera C.**, Bordeasu I., Sălcianu L., Duma S.T., Katona S.E., Punga A., Micu L.M., Pascu L.F., „Considerations regarding the behavior to cavitation erosion of two carbon alloy stainless steels used in the manufacturing of hydraulic equipment drawers of command, adjustment and distribution", HIDRAULICAMagazine of Hydraulics, Pneumatics, Tribology, Ecology, Sensorics, Mechatronics, vol. 1, pp. 25-31, 2015
[13] **Ghera C.**, MiteleaI., BordeasuI., CrăciunescuC.M., „Cavitation erosion behavior of laser nitrided 34CrNiMo6 alloyed steel", METAL 2016 - 25th International Conference on Metallurgy and Materials,Brno, Cehia, pp. 706-711, 2016
[14] Mitelea I., Tillmann W.: „Ştiinţa materialelor", vol. I, Editura Politehnica, Timişoara, 2006
[15] Mitelea I., Tillmann W.: „Ştiinţa materialelor", vol. II, Editura Politehnica, Timişoara, 2007
[16] Mitelea I., **Ghera C.**, Bordeaşu I., Crăciunescu C.M., „Ultrasonic cavitation erosion of a duplex treated 16MnCr5 steel", International Journal of Materials Research, vol. 106, No. 4 , pp. 391-397, April 2015
[17] Mitelea I., **Ghera C.**, Bordeaşu I., Crăciunescu C.M.: „Assement of cavitation errosion of gas-nitrided Cr-Ni-Mo steels", Journal of Tribology ASME, (acceptată pentru publicare), 2017
[18] Oancă O., „Tehnici de optimizare a rezistenţei la eroziunea prin cavitaţie a unor aliaje CuAlNiFeMn destinate execuţiei elicelor navale", Teza de doctorat,Timişoara, 2014
[19] Steller J.K. Giren B.G.: „International Cavitation Erosion Test. Final Report", Gdansk, ISSN 0239-9091, 2015
[20] ***https://www.youtube.com/watch?v=U-uUYCFDTrc,„Cavitation",IETInstitute for Energy Technology, HSR University of Applied Sciences Rapperswil, Switzerland